AGU PUBLICATIONS

Geophysical Research Letters

RESEARCH LETTER

10.1002/2015GL067102

Key Point:

- Strong El Niño greatly increases statewide California wet risk

Supporting Information:

- Tables S1–S8 and captions for Figures S1 and S2
- Figure S1
- Figure S2

Correspondence to:
A. Hoell,
andrew.hoell@noaa.gov

Citation:
Hoell, A., M. Hoerling, J. Eischeid, K. Wolter, R. Dole, J. Perlwitz, T. Xu, and L. Cheng (2016), Does El Niño intensity matter for California precipitation?, *Geophys. Res. Lett.*, *43*, 819–825, doi:10.1002/2015GL067102.

Received 20 NOV 2015
Accepted 8 DEC 2015
Accepted article online 15 DEC 2015
Published online 19 JAN 2016

Does El Niño intensity matter for California precipitation?

Andrew Hoell[1], Martin Hoerling[1], Jon Eischeid[1,2], Klaus Wolter[1,2], Randall Dole[1], Judith Perlwitz[1,2], Taiyi Xu[1,2], and Linyin Cheng[1,2]

[1]Physical Sciences Division, NOAA Earth System Research Laboratory, Boulder, Colorado, USA, [2]Cooperative Institute for Research in Environmental Sciences, University of Colorado Boulder, Boulder, Colorado, USA

Abstract The sensitivity of California precipitation to El Niño intensity is investigated by applying a multimodel ensemble of historical climate simulations to estimate how November–April precipitation probability distributions vary across three categorizations of El Niño intensity. Weak and moderate El Niño events fail to appreciably alter wet or dry risks across northern and central California, though odds for wet conditions increase across southern California during moderate El Niño. Significant increases in wet probabilities occur during strong El Niño events across the entire state. In California's main northern watershed regions, simulations indicate an 85% chance of greater than normal precipitation and a 50% probability of at least 125% of normal. Our results indicate that both the statewide average and the spatial distribution of California precipitation are sensitive to El Niño intensity. Forecasts of El Niño intensity would thus contribute to improved situational awareness for California water planning and related water resource impacts.

1. Introduction

Major statewide California precipitation deficits during water years 2012–2015 rivaled the most intense 4 year droughts in the modern instrumental record [*Griffin and Anchukaitis*, 2014; *Diaz and Wahl*, 2015; *Seager et al.*, 2015]. This multiyear drought produced extensive deleterious impacts on water supplies, wildlife, and ecosystems [*AghaKouchak et al.*, 2015]. El Niño conditions developed in 2015, and as of November 2015, this event ranks within the top three El Niño events extending back to 1950 [*Climate Prediction Center*, 2015a]. A question of great practical interest is how El Niño events of various intensities affect California precipitation [e.g., *Kumar and Hoerling*, 1997; *Hoerling and Kumar*, 1997, 2002; *Zhang et al.*, 2014; *Capotondi et al.*, 2015]. Here we examine potential impacts of El Niño intensity on California precipitation, including both statewide amounts and spatial distributions across northern, central, and southern portions of the state.

Over the period 1896–2014, California precipitation was quite variable from one El Niño event to another. Below average November–April California precipitation was observed during 11 of the 27 El Niño events, including the second driest season on record, which occurred during the weak El Niño of 1923–1924 (Figure 1; cf. Table 1 for a list of events). Above average November–April California precipitation was observed during 16 of the 27 El Niño events, including two of the three wettest seasons, which occurred during the strong events of 1982–1983 and 1997–1998 (Figure 1). The small sample size makes it difficult to draw general conclusions of how El Niño intensity may matter for California precipitation, the hint of strong El Niño flooding events notwithstanding. Given the possibility of another strong El Niño event in winter 2015–2016, it is important to consider the sensitivity of statewide California precipitation to the magnitude of anomalous sea surface temperatures (SSTs) associated with El Niño and how risks of extreme wet or dry conditions may vary across the state in strong El Niños compared with weaker events.

2. Methods and Data

2.1. Observed Data

The observations of California precipitation for November–April 1896–2014 are from the U.S. Climate Divisional Dataset [*Vose et al.*, 2014]. California receives 85% of its annual rainfall during November–April. The observed SSTs are from the merged Hadley-NOAA Optimum Interpolation data set [*Hurrell et al.*, 2008]. Observed SSTs are used to define the occurrences of historical El Niño–Southern Oscillation (ENSO) events and to specify the ocean boundary conditions in historical atmospheric model simulations, hereafter referred to as AMIP after the Atmospheric Model Intercomparison Project [*Gates*, 1992]. El Niño events were also examined in

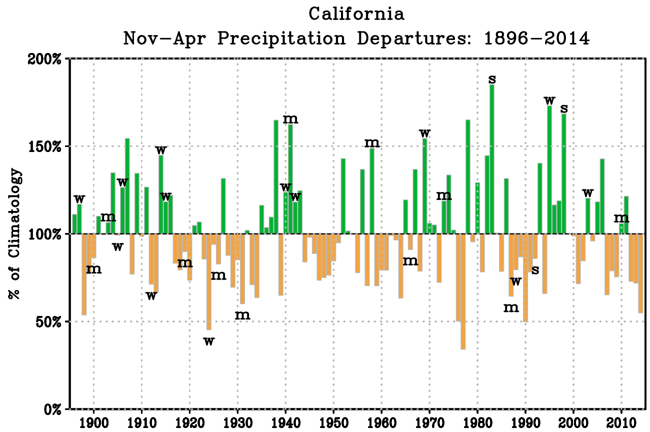

Figure 1. November–April observed statewide California precipitation relative to the long-term mean. s denotes strong El Niño seasons. m denotes moderate El Niño seasons. w denotes weak El Niño seasons.

the ERSST4 data set [*Huang et al.*, 2014] and show a close correspondence with those identified in the SST data set of *Hurrell et al.* [2008].

2.2. Identification of ENSO Categories

ENSO events during November–April 1896–2014 are identified based on a November–April exceedance of SST anomalies in the Niño3.4 region (5°S–5°N, 170°W–120°W) relative to a 1981–2010 climatology. Strong El Niño events are defined when the Niño3.4 index exceeds +1.5°C. Moderate El Niño events are defined when the Niño3.4 index falls between +1.0°C and +1.5°C. Weak El Niño events are defined when the Niño3.4 index falls between +0.5°C and 1.0°C. These El Niño thresholds are the same as those used by the NOAA Climate Prediction Center [*Kousky and Higgins*, 2007; *Climate Prediction Center*, 2015b], although the Climate Prediction Center uses 3 month running means throughout the year instead of the November–April values considered here. A summary of El Niño events for November–April 1896–2014 is presented in Table 1.

There is considerable inter-El Niño event variability in the location of maximum SST anomalies across the tropical Pacific during November–April [*Capotondi et al.*, 2015] (Figure S1 in the supporting information). The SST anomaly expression of the 1982–1983 and 1997–1998 strong El Niño events closely resemble each other in terms of the magnitude of the warm SST anomalies throughout the tropical eastern and central Pacific Ocean. The 1991–1992 El Niño is also notable in terms of November–April Niño3.4 anomaly magnitude, placing it within the strong El Niño category, although the spatial extent of the warmest SST anomalies is not as expansive as 1997–1998 and 1982–1983.

2.3. AMIP Simulations

We examine California precipitation sensitivity using a large ensemble of model simulations because the sample size of observed El Niño events is small. These simulations consist of 130 AMIP runs from three separate models driven by observed monthly time-varying SST, sea ice, greenhouse gases, and ozone for 1979–2014. Descriptions of the three AMIP models and the data used to drive the models are provided in Table S1. This large ensemble makes possible statistically robust estimates of differences in California precipitation responses to three El Niño intensity classes, an exercise not possible from observations alone. The large ensemble of model simulations employed here achieves a better estimate of signal to noise of the California precipitation response to El Niño intensity than the small sample of observations.

2.4. California Precipitation Assessment During El Niño Categories

Composites of observed and simulated precipitation anomalies during November–April of strong, moderate, and weak El Niño are evaluated for all California climate divisions (Figure 2). Observed November–April precipitation composites include the historical period of 1896–2014. Simulated precipitation composites

Table 1. List of El Niño Seasons During 1896–2014[a]

Category	November of Season (Niño3.4 Index)
Strong El Niño	1997 (2.04), 1991 (1.62), 1982 (2.15)
Moderate El Niño	2009 (1.27), 1986 (1.18), 1972 (1.18), 1965 (1.02), 1957 (1.05), 1940 (1.23), 1930 (1.34), 1925 (1.24), 1918 (1.13), 1902 (1.03), 1899 (1.16)
Weak El Niño	2002 (0.95), 1994 (0.80), 1987 (0.54), 1968 (0.69), 1941 (0.70), 1939 (0.79), 1923 (0.52), 1914 (0.55), 1913 (0.67), 1911 (0.88), 1905 (0.77), 1904 (0.57), 1896 (0.97)

[a]The November–April Niño3.4 index anomaly is in parentheses.

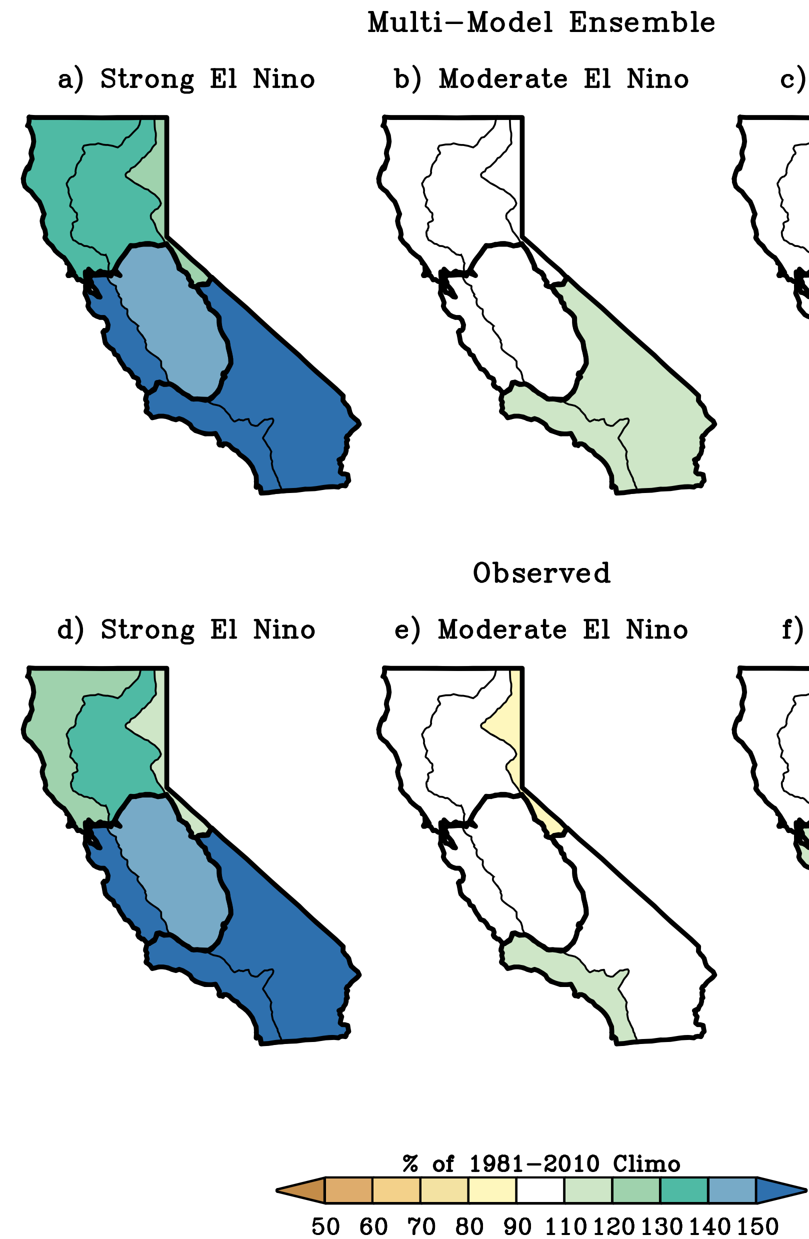

Figure 2. (a–c) Simulated and (d–f) observed November–April average precipitation during strong El Niño (Figures 2a and 2d), moderate El Niño (Figures 2b and 2e), and weak El Niño (Figures 2c and 2f). Thin black lines indicate California climate divisions, and thick black lines indicate northern, central, and southern regions of California.

span the period of 1979–2014 to include the available 130 ensemble members. November–April California precipitation in observation and simulations during El Niño (Figures 2–4) are displayed as a percentage of the average precipitation during 1981–2010.

Precipitation for each of the 130 AMIP ensemble simulations is interpolated to the resolution of California climate divisions using a linear inverse distance squared scheme from the center of the climate division. California is further organized into three regions: northern, central, and southern sections to better discriminate the latitudinal variations of precipitation associated with El Niño impacts (see dark outlines in Figure 2). An area-weighted average is used to calculate the contribution of each California climate division to the northern, central, and southern precipitation. Probability distribution functions (PDFs) and cumulative distribution functions (CDFs) of simulated precipitation are displayed for each El Niño category over the northern, central, and southern California regions in Figures 3 and 4, respectively.

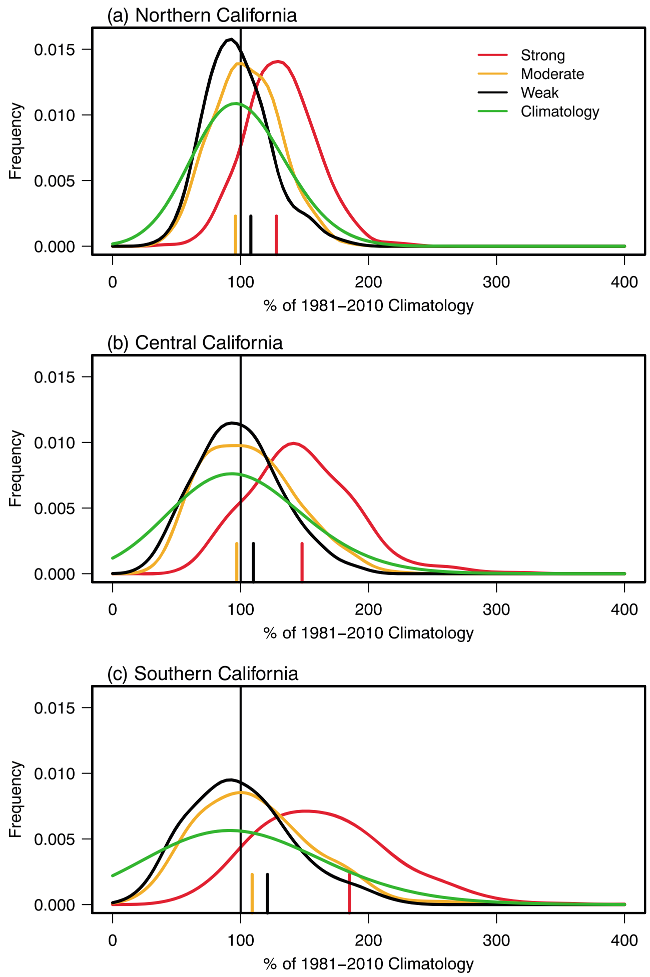

Figure 3. November–April simulated precipitation PDFs separated by El Niño intensity for 1979–2014 over (a) northern, (b) central, and (c) southern California. PDFs for strong El Niño, moderate El Niño, weak El Niño, and all 1981–2010 seasons are shown in red, orange, black, and green, respectively. The red, orange, and black vertical lines indicate the observed mean of the strong El Niño, moderate El Niño, and weak El Niño, respectively. The PDFs were constructed using R software. The PDFs use a nonparametric kernel density estimator that makes no assumptions of normality and a Gaussian smoother. The PDFs are produced using a histogram of 100 bins spanning 0 to 400% so every bin corresponds to 4%. A kernel density estimator with a bandwidth of 3 bins is used to smooth the PDFs.

All 130 ensemble members from the AMIP simulations across the three separate models are aggregated to create a single multimodel ensemble in which each member is weighted equally. The aggregation is justified by the similar mean regional California precipitation during El Niño categories simulated in each model (Tables S2–S4). Though two of the three AMIP models demonstrate a wet bias over each California region (Table S5), the models appear suitable concerning ENSO sensitivity.

3. Results

The ensemble of model simulations indicates acute California precipitation sensitivity to strong El Niño events during November–April (Figures 2a–2c). Strong El Niño results in statewide wet conditions (Figure 2a), moderate El Niño results in wet conditions only over southern California (Figure 2b), and weak El Niño results in statewide near-average precipitation (Figure 2c). The average observed November–April 1896–2014 precipitation separated by El Niño intensity over each California region highlight the distinct difference in conditions during strong El Nino events, analogous to the ensemble average simulations.

We note that the observed composite precipitation for weak El Niño is considerably wetter than for moderate El Niño, especially over southern California. This is likely a symptom of sampling variability rather than an indication of true sensitivity. For instance, among the samples of observed weak El Niño winters are the second driest season on record (1923–1924) and the second wettest season on record (1994–1995) (Figure 1). The model ensemble indicates that moderate El Niño effects are greater than weak El Niño effects consistent with considerations of the tropical forcing and teleconnections [*Hoerling and Kumar*, 2002].

The California precipitation sensitivity to El Niños of various intensities and the spread of possible seasonal precipitation outcomes during individual El Niño events is assessed through PDFs constructed from simulated precipitation during strong, moderate, and weak El Niño (Figure 3). Over northern California, only strong El Niño forces an appreciable change in wintertime precipitation risks, with a virtual elimination of dry probabilities and a dramatic change in tail risks resulting in a near-zero probability of having less than 50% of normal precipitation (Figure 3a). Furthermore, strong El Niño drives a fivefold increase in odds of receiving 150% of the climatological precipitation. These tail risk changes are consistent with an overall shift of the distribution to wet conditions, the mean value of which is roughly one to two standardized departures of the seasonal variability of each model (Table S2). In contrast, the distribution of the simulated

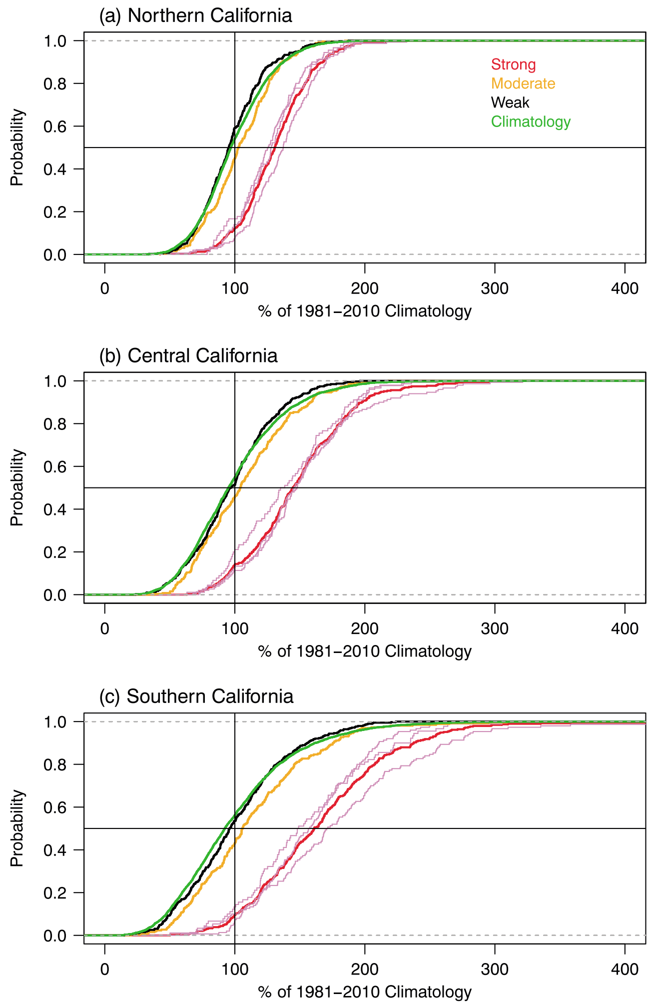

Figure 4. November–April simulated precipitation CDFs separated by El Niño intensity for 1979–2014 over (a) northern, (c) central, and (c) southern California. CDFs for strong El Niño, moderate El Niño, weak El Niño, and all 1981–2010 seasons are shown in red, orange, black, and green, respectively. Thin red lines show the strong El Niño CDFs for each model utilized.

and observed seasonal precipitation statistics shows only a small change for moderate and weak El Niños (Figure 3a).

Likewise, only strong El Niño forces a significant change in wintertime precipitation risks over central California (Figure 3b). The shift in the distribution to wet conditions associated with strong El Niño is roughly two standardized departures of the seasonal variability of each model (Table S3). As such, these results indicate a near-zero probability of less than 75% of normal November–April precipitation (Figure 3b).

Over southern California, even more dramatic sensitivity to strong El Niño during November–April is found, with a median expected departure of 174% (Figure 3c). The shift in the distribution significantly reduces the probability of a dry November–April to less than 10% (Figures 3c and 4c). Moderate El Niño forces a shift in the precipitation distribution to wet conditions, resulting in an increase in mean precipitation to 110% of normal precipitation over southern California (Figure 3c), which is within one standard departure of the seasonal variability (Table S4).

Figure 4 presents CDFs for each of the three California regions to assess probabilities for exceedance of seasonal precipitation during November–April. Consistent with the shift to wet conditions in the PDFs associated with strong El Niño (Figure 3), there are also differences in all threshold exceedance risks during strong El Niño as inferred from the CDFs (thick red curves in Figure 4). The spread in the strong El Niño CDFs between the individual models examined gives confidence in the robustness of the probabilities indicated by the multimodel average (thin red curves in Figure 4). Over the entire state, the simulations indicate a reduced probability of drier than normal precipitation during strong El Niño and an increased probability of receiving greater than 200% of normal.

Such changes in event likelihoods appear plausible, though they are not readily verifiable from the few observations of El Niño during 1979–2014. The observed wet conditions during the strong El Niño are exceedingly low probability outcomes of both moderate and weak El Niño environments. Limited station observations during the strong El Niño event of 1877–1978 reveal that Sacramento, San Francisco, and Red Bluff were each wetter than during 1982–1983 [*Kiladis and Diaz*, 1986]. It is also possible that the models underestimate the probability of very wet winters during non-El Niño years across northern California. For instance, the seventh wettest winter in California was observed in 1937–1938, which was not an El Niño season. This indicates that the AMIP-simulated change in probability exceedance for strong El Niño compared to non-El Niño years may be overstated.

The uncertainty around the tails of the California precipitation distributions is not large for strong, moderate, and weak El Niño (Tables S6–S8). Using a resampling strategy (Figure S2), we find the 95th percentile to be

178% ± 5.7%, 149% ± 5.2%, and 168% ± 6.8% over northern, central, and southern California, respectively. By contrast, we find low confidence for changes in the tail risks for the moderate and weak El Niño intensities. The changes in tail probabilities largely follow from an overall shift in the mean value of the seasonal precipitation distribution, which are much greater during strong El Niños across all portions of California than occurring during either moderate or weak El Niños.

4. Summary and Discussion

The California drought over water years 2012–2015 has resulted in a net statewide precipitation deficit nearly equivalent to the average precipitation falling in one water year, with some parts of the state experiencing net deficits of nearly 2 years rainfall. In addition to these severe Statewide California precipitation deficits, warmer than average near-surface air temperatures during 2012–2015 may have exacerbated the drought [*Diffenbaugh et al*., 2015; *Shukla et al*., 2015; *Williams et al*., 2015] and contributed to reduced water resources available for consumption, increased groundwater withdrawls, and exacerbated agricultural impacts through increased depletion of soil moisture [*California Department of Water Resources*, 2015; *AghaKouchak et al*., 2015]. Here we consider how strong El Niño conditions, such as forecast for winter 2015–2016 [*Climate Prediction Center*, 2015a, 2015b], could affect the probability of a wet November–April rainy season that could at least partially reduce precipitation deficits accumulated during the prolonged severe California drought.

The probability of above average statewide California precipitation during November–April is increased as a result of strong El Niño as compared to moderate and weak El Niño (Figures 2–4). In our simulations, strong El Niño forces a statistically significant shift in the rainfall distributions to wet conditions (Figures 3 and 4). There is some indication that the shape of the seasonal rainfall distributions changes during strong El Niño, with an increased heavy tail.

In a new finding, our experiments indicate that strong El Niño significantly increases the probability of a wetter than average November–April over the principal water supply regions of northern California and the Sierras. The simulations also confirm previous work [e.g., *Ropelewski and Halpert*, 1986; *Schonher and Nicholson*, 1989; *Redmond and Koch*, 1991; *Dettinger et al*., 1998; *McCabe and Dettinger*, 1999] indicating that moderate and weak El Niños do not appreciably modify the probability for wet November–April seasons over the same regions.

Limitations of the present study include the relatively small number of observed cases. The small sample size, particularly for observed strong events, effectively prevents determination of robust statistical distributions of California rainfall based on magnitude alone, especially as there is no physical basis to expect that the magnitude relationship should be linear [see *Hoerling and Kumar*, 2000]. Ensemble simulations can increase sample size to obtain more robust precipitation distributions but are also limited to the extent that they provide realistic responses to SST forcing. In this respect, the broad consistency between observational and model results is reassuring. Our results indicate that the striking agreement between the model mean precipitation response and the three-case observed composite is unlikely due to chance but reflects the heightened sensitivity to strong El Niños. Detectability of the SST-driven signal is high in this case. By contrast, weak signals during weak-moderate El Niños over northern and central California especially lead to low detectability. There is thus an increased risk of confounding sampling noise with El Niño impacts in observational composites based on small sample size.

In order to strengthen confidence in the results, greater understanding is also required of physical mechanisms by which El Niño effects on California rainfall. Of particular importance is clarification of the physical mechanisms by which the magnitude and position of their SST anomalies [*Capotondi et al*., 2015] drive both regional jet stream and teleconnection responses, as well as any indirect effects on the evolution midlatitude storm systems and phenomena such as atmospheric rivers that contribute to the majority of California's winter precipitation [*Larkin and Harrison*, 2005; *Yu et al*., 2012; *Chiodi and Harrison*, 2012].

Acknowledgments
The authors thank the NOAA Climate Program Office for support, Daithi Stone and Michael Wehner of the Computational Research Division at the Lawrence Berkeley National Laboratory for access to CAM5 simulations, anonymous reviewers for their thoughtful and helpful comments, and Shrad Shukla for useful feedback on an earlier version of the manuscript.

References

AghaKouchak, A., D. Feldman, M. Hoerling, T. Huxman, and J. Lund (2015), Water and climate: Recognize anthropogenic drought, *Nature*, *524*(7566), 409–411, doi:10.1038/524409a.

California Department of Water Resources (2015), Drought in California, State of California. [Available at http://www.water.ca.gov/water-conditions/docs/DWR_DroughtBroch_070815-web.pdf.]

Capotondi, A., et al. (2015), Understanding ENSO diversity, *Bull. Am. Meteorol. Soc.*, *96*, 921–938, doi:10.1175/BAMS-D-13-00117.1.

Chiodi, A. M., and D. E. Harrison (2012), El Niño impacts on seasonal U.S. atmospheric circulation, temperature, and precipitation anomalies: The OLR-event perspective*, *J. Clim.*, *26*(3), 822–837, doi:10.1175/JCLI-D-12-00097.1.

Climate Prediction Center (2015a), November 2015 ENSO Diagnostic Discussion. [Available at http://www.cpc.ncep.noaa.gov/products/expert_assessment/ENSO_DD_archive.shtml.]

Climate Prediction Center (2015b), Keep calm and stop obsessing over weekly changes in ENSO. [Available at https://www.climate.gov/news-features/blogs/enso/keep-calm-and-stop-obsessing-over-weekly-changes-enso.]

Dettinger, M. D., D. R. Cayan, H. F. Diaz, and D. M. Meko (1998), North-south precipitation patterns in western North America on interannual-to-decadal timescales, *J. Clim.*, *11*(12), 3095–3111, doi:10.1175/1520-0442(1998)011<3095:NSPPIW>2.0.CO;2.

Diaz, H. F., and E. R. Wahl (2015), Recent California water year precipitation deficits: A 440-year perspective, *J. Clim.*, *28*(12), 4637–4652, doi:10.1175/JCLI-D-14-00774.1.

Diffenbaugh, N. S., D. L. Swain, and D. Touma (2015), Anthropogenic warming has increased drought risk in California, *Proc. Natl. Acad. Sci. U.S.A.*, *112*(13), 3931–3936.

Gates, W. L. (1992), AMIP: The Atmospheric Model Intercomparison Project, *Bull. Am. Meteorol. Soc.*, *73*(12), 1962–1970, doi:10.1175/1520-0477(1992)073<1962:ATAMIP>2.0.CO;2.

Griffin, D., and K. J. Anchukaitis (2014), How unusual is the 2012–2014 California drought?, *Geophys. Res. Lett.*, *41*, 9017–9023, doi:10.1002/2014GL062433.

Hoerling, M. P., and A. Kumar (1997), Why do North American climate anomalies differ from one El Niño event to another?, *Geophys. Res. Lett.*, *24*(9), 1059–1062, doi:10.1029/97GL00918.

Hoerling, M. P., and A. Kumar (2000), Understanding and predicting extratropical teleconnections related to ENSO, in *El Niño and the Southern Oscillation: Multi-Scale Variability, and Global and Regional Impacts*, edited by H. F. Diaz and V. Markgra, pp. 57–88, Cambridge Univ. Press, Cambridge, U. K.

Hoerling, M. P., and A. Kumar (2002), Atmospheric response patterns associated with tropical forcing, *J. Clim.*, *15*(16), 2184–2203, doi:10.1175/1520-0442(2002)015<2184:ARPAWT>2.0.CO;2.

Huang, B., V. F. Banzon, E. Freeman, J. Lawrimore, W. Liu, T. C. Peterson, T. M. Smith, P. W. Thorne, S. D. Woodruff, and H.-M. Zhang (2014), Extended reconstructed sea surface temperature version 4 (ERSST.v4). Part I: Upgrades and Intercomparisons, *J. Clim.*, *28*(3), 911–930, doi:10.1175/JCLI-D-14-00006.1.

Hurrell, J. W., J. J. Hack, D. Shea, J. M. Caron, and J. Rosinski (2008), A new sea surface temperature and sea ice boundary dataset for the Community Atmosphere Model, *J. Clim.*, *21*(19), 5145–5153, doi:10.1175/2008JCLI2292.1.

Kiladis, G. N., and H. F. Diaz (1986), An analysis of the 1877–78 ENSO episode and comparison with 1982–83, *Mon. Weather Rev.*, *114*(6), 1035–1047, doi:10.1175/1520-0493(1986)114<1035:AAOTEE>2.0.CO;2.

Kousky, V. E., and R. W. Higgins (2007), An alert classification system for monitoring and assessing the ENSO cycle, *Weather Forecasting*, *22*(2), 353–371, doi:10.1175/WAF987.1.

Kumar, A., and M. P. Hoerling (1997), Interpretation and implications of the observed inter-El Niño variability, *J. Clim.*, *10*(1), 83–91, doi:10.1175/1520-0442(1997)010<0083:IAIOTO>2.0.CO;2.

Larkin, N. K., and D. E. Harrison (2005), On the definition of El Niño and associated seasonal average U.S. weather anomalies, *Geophys. Res. Lett.*, *32*, L13705, doi:10.1029/2005GL022738.

McCabe, G. J., and M. D. Dettinger (1999), Decadal variations in the strength of ENSO teleconnections with precipitation in the western United States, *Int. J. Climatol.*, *19*(13), 1399–1410, doi:10.1002/(SICI)1097-0088(19991115)19:13<1399::AID-JOC457>3.0.CO;2-A.

Redmond, K. T., and R. W. Koch (1991), Surface climate and streamflow variability in the western United States and their relationship to large-scale circulation indices, *Water Resour. Res.*, *27*(9), 2381–2399, doi:10.1029/91WR00690.

Ropelewski, C. F., and M. S. Halpert (1986), North American precipitation and temperature patterns associated with the El Niño/Southern Oscillation (ENSO), *Mon. Weather Rev.*, *114*(12), 2352–2362, doi:10.1175/1520-0493(1986)114<2352:NAPATP>2.0.CO;2.

Schonher, T., and S. E. Nicholson (1989), The relationship between California rainfall and ENSO events, *J. Clim.*, *2*(11), 1258–1269, doi:10.1175/1520-0442(1989)002<1258:TRBCRA>2.0.CO;2.

Seager, R., M. Hoerling, S. Schubert, H. Wang, B. Lyon, A. Kumar, J. Nakamura, and N. Henderson (2015), Causes of the 2011 to 2014 California drought, *J. Clim.*, *28*, 6997–7024, doi:10.1175/JCLI-D-14-00860.1.

Shukla, S., M. Safeeq, A. AghaKouchak, K. Guan, and C. Funk (2015), Temperature impacts on the water year 2014 drought in California, *Geophys. Res. Lett.*, *42*, 4384–4393, doi:10.1002/2015GL063666.

Vose, R. S., S. Applequist, M. Squires, I. Durre, M. J. Menne, C. N. Williams, C. Fenimore, K. Gleason, and D. Arndt (2014), Improved historical temperature and precipitation time series for U.S. climate divisions, *J. Appl. Meteorol. Climatol.*, *53*(5), 1232–1251, doi:10.1175/JAMC-D-13-0248.1.

Williams, A. P., R. Seager, J. T. Abatzoglou, B. I. Cook, J. E. Smerdon, and E. R. Cook (2015), Contribution of anthropogenic warming to California drought during 2012–2014, *Geophys. Res. Lett.*, *42*, 6819–6828, doi:10.1002/2015GL064924.

Yu, J.-Y., Y. Zou, S. T. Kim, and T. Lee (2012), The changing impact of El Niño on US winter temperatures, *Geophys. Res. Lett.*, *39*, L15702, doi:10.1029/2012GL052483.

Zhang, T., J. Perlwitz, and M. P. Hoerling (2014), What is responsible for the strong observed asymmetry in teleconnections between El Niño and La Niña?, *Geophys. Res. Lett.*, *41*, 1019–1025, doi:10.1002/2013GL058964.